Dynamic Analysis of Motion of Crawler-Type Remotely Operated Vehicles

Tomoya Inoue, *Member, IEEE*, Takuya Shiosawa, and Ken Takagi, *Member, IEEE*

***Abstract*—A crawler system has the potential to expand research and development on seafloors with irregular steep terrain and sand. Characteristic parameters in water, such as added mass, buoyancy, and hydrodynamic forces, considerably affect and decrease the mobility of crawler-type remotely operated vehicles (ROVs). To study and evaluate the mobile performance of a crawler system, it is important to investigate the dynamic motion of the crawler system by considering these effects. This paper presents a mathematical model of an underwater crawler system to show the dynamic effects on the vehicle's motion; experiments were conducted on a crawler-type ROV climbing over a bump in a water tank to examine the slip characteristics at sea. The simulated results agreed well with the experimental results. The mathematical model presented in this paper simulates the dynamic motion for climbing over a bump and the slip characteristics very well, and it reveals the physics of the crawler-type ROV's motion. The proposed mathematical model is useful for dynamic analysis.**

***Index Terms*—Crawler remotely operated vehicle (ROV), dynamic analysis, slip characteristics.**

I. Introduction

REMOTELY OPERATED VEHICLES (ROVs) are being used to conduct research or work on flat, even seafloors and in water, and the activity in these environments is expected to be expanded. Recently, underwater exploration has gained attention so as to exploit underwater mineral resources such as hydrothermal deposit areas. This requires ROVs to work on seafloors with irregular, steep terrain. Hydrothermal deposits are contained in steep terrain having slopes of more than 30° in some areas, and the seafloor can be bumpy with assumed irregularities of 20–50 cm. To conduct work or survey operations there, ROVs need functions to move and bear the reaction force of operations. In addition, ROVs sometimes need to remain stationary and keep their posture stable during operations such as coring, which is an important issue [1]. Conventional ROVs, such as those that hover, generally bear the reaction force by their weight or thrusters. However, this is sometimes insufficient for bearing large forces, which limits operation. Although conventional ROVs equip thrusters to move in water, they do not have the function of moving on the seafloor.

Manuscript received August 03, 2011; revised August 23, 2012; accepted October 11, 2012. Date of publication February 01, 2013; date of current version April 10, 2013.

Guest Editor: W. Kirkwood.

T. Inoue is with JAMSTEC CDEX, Yokohama, Kanazawa-ku 236-0001, Japan (e-mail: inouet@jamstec.go.jp).

T. Shiosawa is with Kawasaki Heavy Industries, Ltd., Kobe, Hyogo 650-8670, Japan.

K. Takagi is with The University of Tokyo, Tokyo 113-0033, Japan (e-mail: takagi@k.u-tokyo.ac.jp).

Color versions of one or more of the figures in this paper are available online at http://ieeexplore.ieee.org.

Digital Object Identifier 10.1109/JOE.2012.2225292

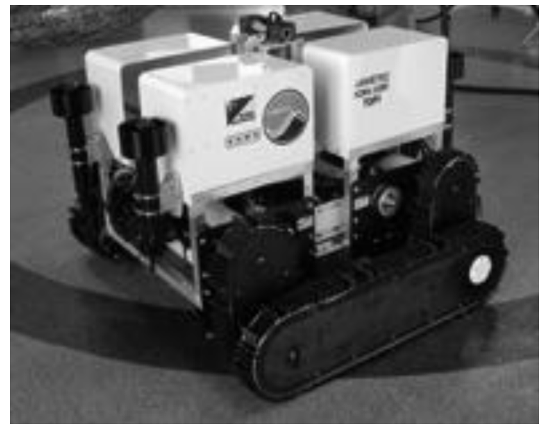

Fig. 1. Picture of a crawler-type ROV.

A possible advanced function for an ROV to operate on the seafloor is a crawler system. Underwater crawlers have been developed [2]–[7]. However, their activities and working area are still limited because they were designed for a specific area, such as the coast or shallow sandy seafloors, which are not irregular terrains.

To expand research and development on the seafloor—for surveying, sampling, or working on irregular terrain—an advanced mobility function needs to be developed. Inoue *et al.* [8] developed the flipper-type crawler system shown in Fig. 1. The flipper-type crawler has an additional function for rotating itself, which improves its mobility on seafloors with irregular terrain, and also it enables the posture of the ROV to be actively changed or maintained.

The objective of this study is to improve the mobility of an ROV on a variety of seafloors such as sand, rock reefs with inclinations of more than 30°, and seafloor covered with cobbles or gravel 10–50 cm in size. Inoue *et al.* [8], [9] conducted experiments in a water tank and at sea. They confirmed that the flipper-type crawler system has advantages in performance: it has the potential to operate on seafloors with irregular steep terrain and climb over bumps higher than those climbed over by a conventional crawler system. On the other hand, the experiments also showed that the ROV would do a wheelie, i.e., bow-up running, as shown in Fig. 2, and that the ROV slipped and, in extreme cases, sunk into the sandy seafloor [9]. Thus, examining an ROV's mobility, particularly its stable running and slip characteristics, via experimental and theoretical approaches, is necessary.

There have been several studies on the mobile characteristics of a crawler on land [10], [11]. However, there has been

Fig. 2. Picture of a crawler-type ROV performing a wheelie.

insufficient research on the mobility characteristics of underwater crawlers, even though underwater crawlers have been developed and autonomous control has been attempted [12], [13]. Yoshida *et al.* [14] and Endo *et al.* [15] pointed out the importance of the slip characteristics and considered it in a trajectory control model as an unknown parameter that was estimated from the actual measurement during operation.

The difference in the mobility of a crawler on land and underwater is due to the hydrodynamic effect, which includes the added mass, buoyant force, and center of buoyancy. Inoue *et al.* [9], [16] and Katsui *et al.* [17], [18] examined the equilibrium during operation considering the hydrodynamic influence and showed that, in water, the equilibrium operating characteristics of the crawler system are lower than those on land because of the buoyant force, including the effect of the center of buoyancy. This means that an ROV with a crawler system tends to wheelie 脱离地面 more in water than on land. These investigations examined operation not only on a flat, even seafloor but also on a steep seafloor, while climbing over a bump. Inoue *et al.* [9], [16] and Katsui *et al.* [17], [18] presented discriminant criteria derived from a static analysis that considers the gravity, buoyancy, and centers of buoyancy for preventing wheelies during a steady running motion. Inoue *et al.* [19] proposed utilizing vertical thrusters to expand possible running conditions without wheelies using the discriminant criteria. The investigation was conducted using static and quasi-static analysis, and they reported the importance of dynamic effects because wheelies occur during the initial acceleration.

The other important mobility characteristic is the slip 滑动, as mentioned above; slip is the difference in speeds of the ROV and the crawler belt. The slip is affected by the friction between the crawler belt and the seafloor, vehicle speed, acceleration, weight in water, and hydrodynamic forces such as the drag force and the added mass. These parameters should be characterized in water and are different from those on land. The above studies reported larger slips and attitude variations for the crawler system in water than on land. These works used static analysis to demonstrate differences between crawler-type ROV motions in water and on land. However, dynamic analysis of the crawler-type ROV motion is clearly necessary to understand the physics, particularly for accelerated motions.

Shiosawa *et al.* [20] proposed a mathematical formulation of the crawler-type ROV motion, and this formulation was partially validated by Inoue *et al.* [21] via experimental results on the mobility performance and effect of parameters in water. These researchers used the lumped mass method for the mathematical formulation of the crawler belt, in which the crawler is modeled as a massless linear spring and a finite number of mass points. The crawler-type ROV shown in Fig. 1 was used in the experiment; its mobility was observed, and the slip was measured.

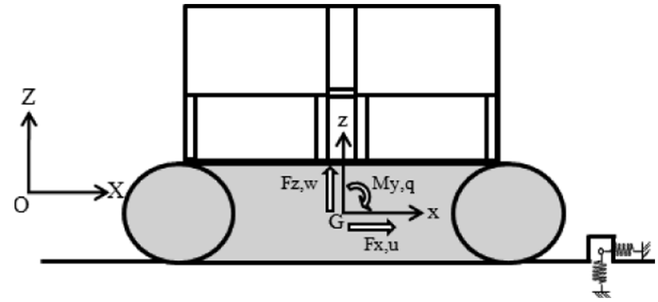

Fig. 3. Coordinate system and mathematical model of a crawler-type ROV.

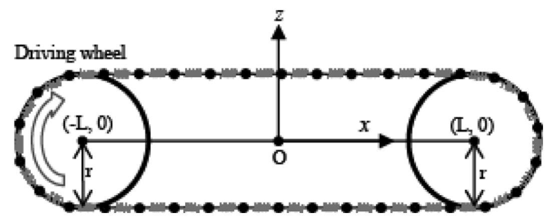

Fig. 4. Mathematical model of the crawler belt.

This paper presents an improved numerical scheme that uses soil test results based on sand collected from the actual sea and discusses the numerical and experimental results.

II. Mathematical Formulation

Characteristic parameters in water, such as buoyancy and hydrodynamic forces, considerably affect and decrease the mobility and acceleration of crawler-type ROVs. In addition, the friction force between the crawler belt and the seafloor is completely different from that on land. This means that the running model of a crawler on land is not directly applicable to crawler-type ROVs in water. Thus, it is necessary to establish a mathematical model to express the motion performance of an underwater crawler system that considers the parameters mentioned above.

Shiosawa *et al.* [20] proposed a mathematical model for investigating the dynamic motion of a crawler-type ROV. This section briefly presents a formulation of their model.

The coordinate system is shown in Fig. 3. The crawler-type ROV shown in Fig. 1 was analyzed in this study. An ordinary crawler was analyzed for the sake of simplicity, although the crawler-type ROV shown in Fig. 1 also has a flipper crawler. The method can be extended to the flipper crawler system.

A. Mathematical Model of the Crawler Belt

The crawler belt is assumed to be represented by a set of discrete masses interconnected by massless linear springs, as illustrated in Fig. 4. The external forces acting on a crawler belt are the body force including gravity, line tension, the normal component of the reaction force, and the external force necessary for maintaining the crawler's velocity.

For actual operation of the crawler, drive motors are controlled to maintain the rotation speed by using a feedback system. Thus, the motion of a driven wheel should be included in the system of crawler motion equations where the driving force from the drive motors is controlled by the feedback system. In this study, the rotation speed of the drive heel was treated as an input parameter for the sake of simplicity.

The equations of motion for the ith lumped mass are as follows:

$$m\ddot{x}_j = a_{xj}T_j + b_{xj}T_{j-1} + c_{xj}R_j + d_{xj}F_j + G_{xj} \quad (1)$$

$$m\ddot{z}_j = a_{zj}T_j + b_{zj}T_{j-1} + c_{zj}R_j + d_{zj}F_j + G_{zj} \quad (2)$$

where m is the mass of the jth lump; $\ddot{x}_j$ and $\ddot{z}_j$ are the accelerations of the jth lumped mass in the x- and z-directions, respectively; T_j is the tension in the segment between the jth and $(j+1)$th lumped masses; R_j is the normal component of reaction in the jth lumped mass; F_j is the external force to keep velocity in the jth lumped mass; G_{xj} and G_{zj} are body forces in the jth lumped mass; $a_{xj}, b_{xj}, c_{xj},$ and d_{xj} are functions of x_j determined by the configuration of the lumped masses; and $a_{zj}, b_{zj}, c_{zj},$ and d_{zj} are functions of z_j determined by the configuration of the lumped masses.

Additional constraint equations—the geometric restraint on the wheels and the elongation rigidity of the crawler belt—are given as

$$(x_j - L)^2 + y_j^2 = r^2, (|x| \geq L) \quad (3)$$

$$(x_j - x_{j+1})^2 + (z_j - z_{j+1})^2 = dL^2\left(1 + \frac{T_j}{AE}\right). \quad (4)$$

The equations are integrated using Houbolt's method. Details are in [20].

B. Mathematical Model of Motion of the Main Body

The motions of the ROV are expressed as (5), shown at the bottom of the page, where M is the mass of the main body; A_{ij} is the added mass for the ith mode because of the jth mode motion; u and w are velocity components of the main body in the x- and z-directions; q is the angular velocity of the main body; F_{GX} and F_{GZ} are frictions of the seafloor; T_{GY} is the rotating torque; Z_{qq} and M_{qq} are hydrodynamic derivatives of the main body with respect to angular velocity; $X_{kk}, Z_{kk},$ and M_{kk} are hydrodynamic derivatives of the main body with respect to velocity $(k = u, w)$; θ is the Eulerian angle of the main body; ρ is water density; and ∇ is the displacement of the main body.

C. Hydrodynamic Forces

The added masses A_{11}, A_{33}, A_{15}, A_{51}, and A_{55}, are calculated via the 3-D boundary element method, which is a well-known method for the numerical simulation of hydrodynamic forces. They are nondimensionalized to the length and width of the main body. The hydrodynamic derivatives are assumed to be drag forces, and the measured values are used; drag coefficients C_{dx}, C_{dy}, and C_y are shown in Table I.

TABLE I
ADDED MASS AND DRAG COEFFICIENTS OF THE MAIN BODY

Items	Nondimensional added mass and drag coefficient
A'_{11}	0.594
A'_{33}	0.919
A'_{15}, A'_{51}	0.165
A'_{55}	0.059
C_{dx}	1.02
C_{dy}	1.53
C_y	0.013

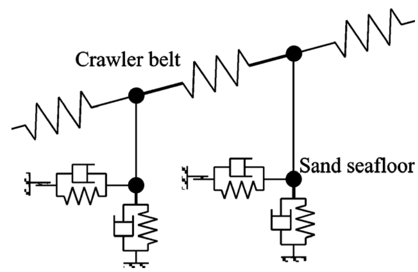

Fig. 5. Mathematical model of a crawler belt and sand seafloor.

D. Mathematical Model of the Seafloor

Interaction between the crawler belt and the seafloor is represented by adding reaction forces onto the lumped mass of the crawler belt from the seafloor. Abe *et al.* [10] presented a mathematical model for a metal crawler belt on land, which represents the reaction force as a distribution along a spring and damper system, as shown in Fig. 5.

In their model, the vertical component of the reaction force is modeled by a spring and a dashpot in parallel; this is commonly called Voigt's model. The relationship between sinkage z and contact pressure P_s is obtained using Bekker's equation [22] with the coefficient of sinkage K_{SI} and sinkage index n, which are determined according to the properties of the seafloor

$$ps = K_{SI}z^n. \quad (6)$$

Thus, the spring constant in the vertical direction is obtained.

The relationship between the shear strain and the shear stress of sand is linear when the deformation is elastic, and the shear deformation suddenly increases when the shear stress exceeds

$$\begin{bmatrix} M + A_{11} & 0 & A_{15} \\ 0 & M + A_{33} & 0 \\ A_{51} & 0 & M + A_{55} \end{bmatrix} \cdot \begin{bmatrix} \dot{u} \\ \dot{w} \\ \dot{q} \end{bmatrix} = \begin{bmatrix} -(M + A_{33})qw + (M - \rho\nabla)g\sin\theta + X_{uu}u^2 + X_{ww}w^2 + F_{GX} \\ (M + A_{11})qw + A_{15}q^2 - (M - \rho\nabla)g\cos\theta + Z_{ww}w^2 + Z_{qq}q^2 + Z_w w + F_{GZ} \\ A_{15}qw - (A_{11} - A_{33})uw + M_w w^2 + M_{ww}w^2 + M_{qq}q^2 + T_{GY} \end{bmatrix} \quad (5)$$

TABLE II
SPECIFICATIONS OF THE CRAWLER-TYPE ROV

Items	
Dimensions	[L] 652 mm × [B] 764 mm × [H] 530 mm
Max. Power of motor	4 × 150 W
Weight	580 N in air

the critical shear stress. Abe *et al.* [10] used the Coulomb equation to represent the critical shear stress, and they represented the spring coefficient of the shear stress as a linear equation of the contact pressure

$$k_{SH}(z) = K_{CO} + p_s K_{sp} = K_{CO} + K_{SI} z^n K_{sp} \quad (7)$$

where K_{CO} and K_{sp} are constants.

Abe *et al.* [10] concluded that their mathematical model agreed well with the experimental results on determining all the coefficients that appeared in their mathematical model via a conventional soil test.

In this study, the spring and damper system was used in the same manner as in Abe *et al.*'s model. However, the same spring coefficient of the reaction force cannot be used because of the following reasons. First, deformation of the crawler belt is expected because the belt is made of rubber. Second, soil properties in water, particularly for sandy seafloor, are not well known. Thus, for the sake of simplicity, the contact pressure was assumed to be proportional to the reaction force, i.e., $n = 1$, and the critical shear force was evaluated using the static friction coefficient.

Measurement of the sand characteristics for the mathematical model of the seafloor as discussed above was carried out in the laboratory using real sand collected from the seafloor off Kohama-jima, where the slip was measured. The measured spring constant for the vertical reaction force and the spring constant for the shear stress are represented by the static and kinematic friction coefficients of 0.6 and 0.5, respectively. Since there is no available mathematical model for the damping coefficient, the damping coefficient was chosen so that the numerical results would not show any unrealistic vibration.

III. EXPERIMENTS

Experiments were conducted with the crawler-type ROV both at sea and in a water tank to investigate its performance when climbing over a bump and its slip characteristics. It is noted that a dual-flipper system is equipped on the ROV used in the experiment, as shown in Fig. 1. The dual-flipper was folded and not used during the experiments to match the theoretical work. Table II shows the specifications of the crawler-type ROV used for the experiment.

A. Climbing Over a Bump

To investigate the climbing ability of the crawler-type ROV, a step was placed in the water tank. The crawler-type ROV ran over it, as shown in Fig. 6. Experiments were carried out for two steps with different heights, running speeds, and the center of buoyancy.

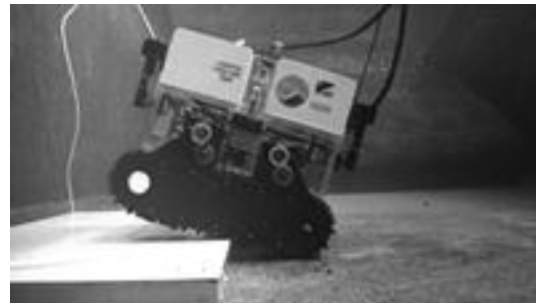

Fig. 6. Picture of the experiment showing the crawler-type ROV climbing over a step in the water tank.

Fig. 7 shows examples of the attitude of the main body as it ran and climbed over a step with a height of 65 mm where the weight of the ROV in water was 191 N. The rates of revolution of the drive motor were 1500, 3000, and 4500 r/min, corresponding to crawler belt speeds of 0.149, 0.297, and 0.446 m/s, respectively. The attitude of the ROV was measured by a gyro system equipped on the ROV. The rotation speed changed when the load on the crawler belt was high, because the drive motor had no feedback control system. Fig. 7(a) shows the results for when the center of buoyancy was at the center in the longitudinal direction. Fig. 7(b) shows the results for when the center of buoyancy was moved forward by relocating the buoyancy materials. The results show that the attitude of the ROV is affected by its speed and the center of buoyancy position.

B. Slip Characteristics

The experiment for examining the slip characteristics of the ROV was conducted both in the water tank and at sea. In the tank test, a wooden flat plate was used as a seafloor. The experiment at sea was conducted off the coast of Kohama-jima, Okinawa, Japan. Fig. 8 shows a picture of this experiment. The weight in water was varied in the experiment. The motions of the main body and the crawler belt were captured by a video camera system, which appears in Fig. 8(b), and their velocity was obtained by differentiating the motion.

Fig. 9 shows an example of the horizontal motion in the experiment when the crawler belt was accelerated from 0 to 0.5 m/s in 0.8 s. The acceleration of the crawler belt up to 0.8 s seemed almost linear; however, there were some fluctuations. Two reasons can explain the fluctuations: the rotation of the drive motor did not constantly accelerate because of the lack of feedback control, and the velocity measurement was not accurate enough because it was obtained by differentiating the motion as captured by a video camera system.

There was clearly a slip between the crawler belt and the seafloor, because the ROV speed was certainly less than the belt speed and the motion of the ROV itself was separate from the crawler belt. This difference became small when the acceleration was small.

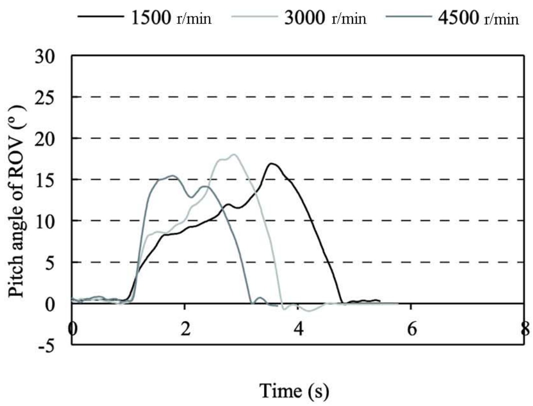

(a)

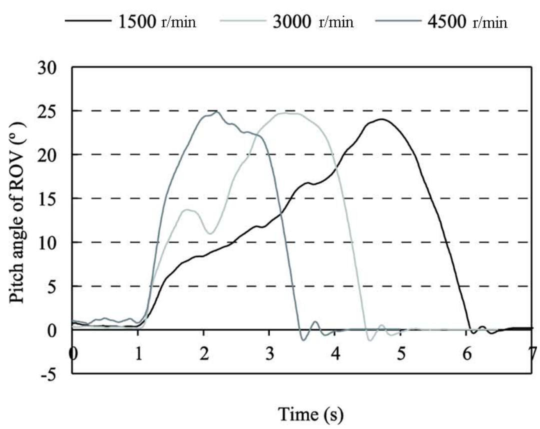

(b)

Fig. 7. Attitude of the ROV when running and climbing over the bump.

(a) (b)

Fig. 8. Pictures of the slip measurement at sea.

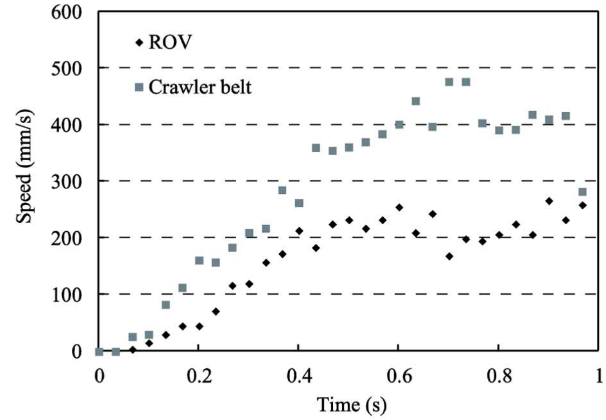

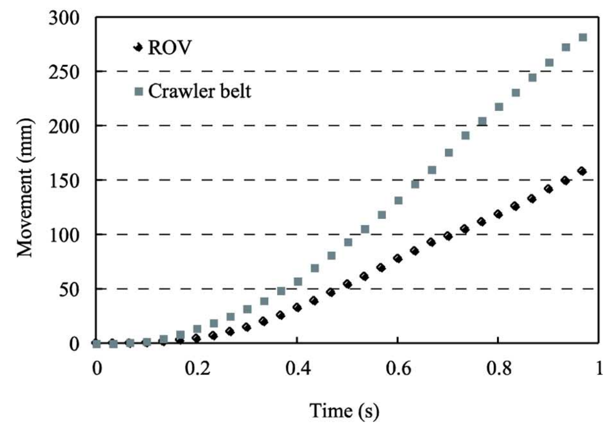

Fig. 9. Experimental results for horizontal velocity and displacement of weight in water of 98 N.

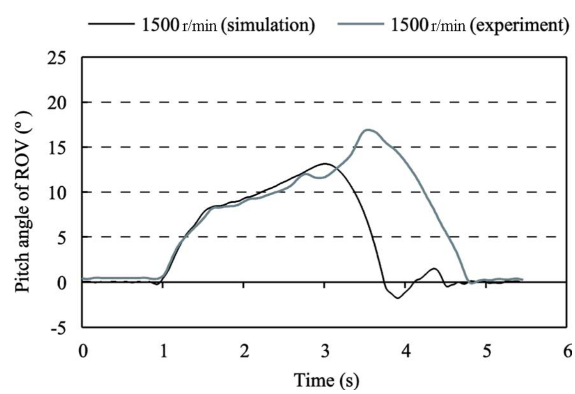

Fig. 10. Comparison of pitch angles obtained from the experiment and the simulation for an ROV running and climbing over a bump at a revolution rate of 1500 r/min.

IV. Comparison Between Experimental and Simulation Results

A. Climbing Over a Bump

A computer code was developed based on the mathematical model presented in Section III to simulate the climbing and slip motions. Fig. 10 shows a sample comparison between the simulation and the experiment. The angle presented here is the pitch angle of the ROV. The conditions are as follows: weight in water of 191 N, revolution rate for the drive motor of 1500 r/min, initial speed of 0.149 m/s, and step height of 65 mm.

The simulated result agrees well with the experimental result, except for the last stage of climbing over the bump. This is because, in the last stage, the ROV has already climbed up the step, and the pitch angle decreased. In this case, the influence of the floor on the pitch added mass and drag coefficient became large, which prevented the pitch angle from decreasing; however, this effect was not considered in the mathematical model. Thus, the pitch angle in the simulation decreased faster than that in the experiment.

Fig. 11 shows the same comparison but with a different initial speed of the ROV. The revolution rate of the drive motor was 3000 r/min, and the initial speed was 0.297 m/s. The simulated result shows a peak, whereas the experimental result was flat when the ROV started to climb up the step. This is because the drive motor could not maintain a constant rate of revolution when a large torque of the drive motor was necessary, because of the lack of a feedback system.

This implies that the dynamic model of the drive motor and its gear train system should be considered for further improvement

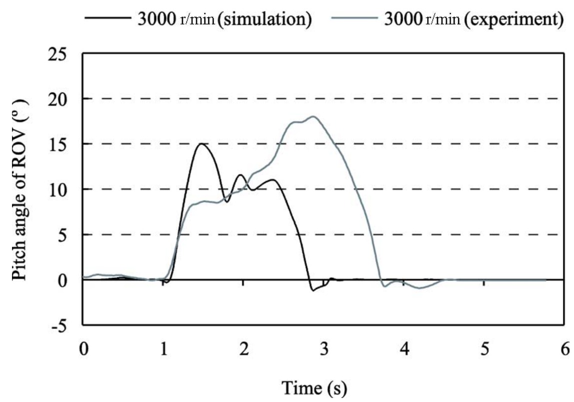

Fig. 11. Comparison of pitch angles obtained from the experiment and the simulation for an ROV running and climbing over a bump at a revolution rate of 3000 r/min.

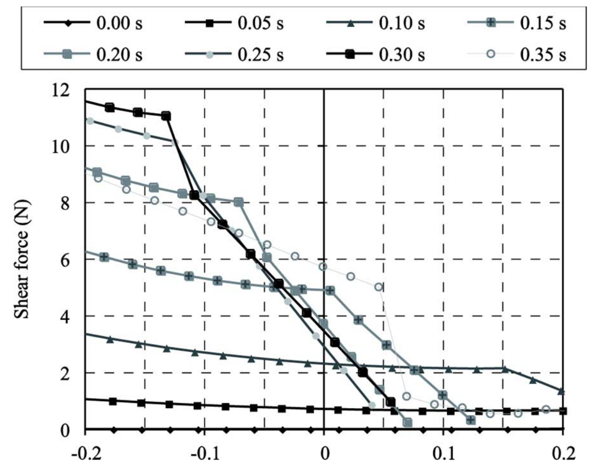

Fig. 13. Shear stress distribution along the crawler belt with time.

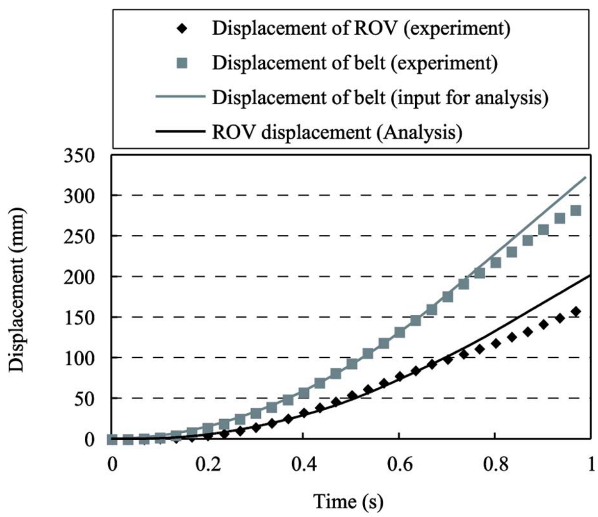

Fig. 12. Comparison between the calculated and experimental horizontal displacements for an acceleration of 0.62 m/s^2 and weight in water of 98 N.

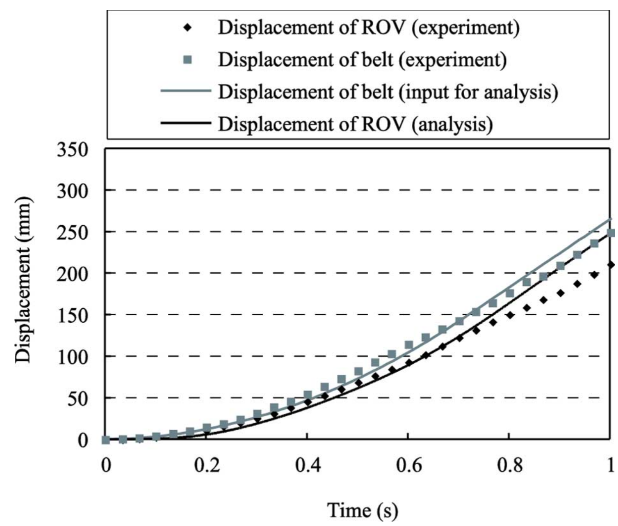

Fig. 14. Comparison between the calculated and experimental horizontal displacements for an acceleration of 0.62 m/s^2 and weight in water of 392 N.

of this method as well as improvement of the hydrodynamic model for the last stage of climbing over an obstacle.

B. Slip Characteristics

Slip is defined as the difference between the horizontal displacements of the crawler belt and the main body of the ROV. Fig. 12 shows the comparison between the experimental and calculated results for the horizontal displacements.

The calculated result clearly agrees with the experimental result. On the other hand, the horizontal displacement of the main body is separate from that of the crawler belt. This is because the shear stress under the crawler belt partially exceeds the critical shear stress, and thus, the slip between the crawler belt and the seafloor occurs. However, this phenomenon is not simple, because the contact pressure under the crawler belt is affected by the moment of inertia of the main body because of the acceleration as well as the weight in water. Fig. 13 shows the distribution of the shear stress along the crawler belt, which was obtained from the simulation results for the crawler belt and (6) and (7).

The shear stress is clearly not homogeneous in space or time. For example, at $t = 0.25$, the aft part of the crawler belt does not slip since the reaction force there is high enough because of the moment of inertia due to acceleration of the main body, whereas the fore part of the crawler slips. The slip length also clearly varies over time. It is noted that Fig. 13 cannot be obtained by the quasi-static method; dynamic analysis is important for understanding slip phenomena.

Since the acceleration of the ROV and the weight in water were supposed to be major parameters of the slip characteristics, other experiments with different accelerations and weights were also carried out. Fig. 14 compares the calculated and experimental results for horizontal displacements at an acceleration of 0.62 m/s^2 and weight in water of 392 N. The slip was found to decrease as the weight in water increased.

Fig. 15 compares the calculated and experimental results for horizontal displacements at an acceleration of 0.16 m/s^2 and weight in water of 98 N. The slip was small when the acceleration was small.

Based on the above discussion, plots of the experiment results with differing weight and acceleration values would be helpful.

Fig. 16 summarizes the slip characteristics by showing slip ratios for different accelerations. The slip ratio is defined as the ratio of slip to the speed of the crawler belt, where the slip ratio is obtained just after stop acceleration. The results show that the

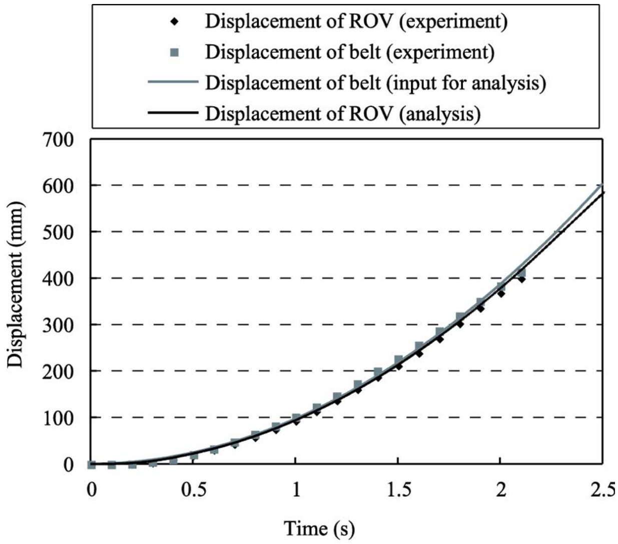

Fig. 15. Comparison between the calculated and experimental horizontal displacements for an acceleration of 0.18 m/s^2 and weight in water of 98 N.

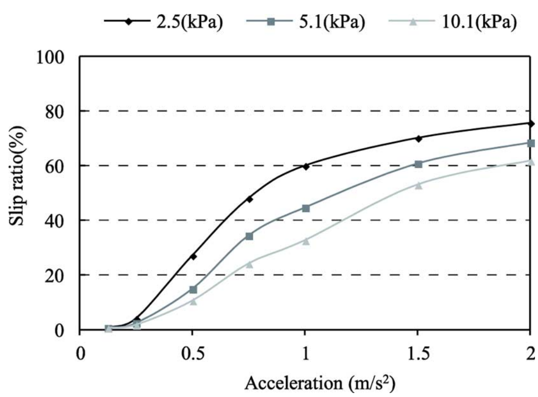

Fig. 16. Slip ratio with respect to crawler drive acceleration and ground pressure variations.

slip ratio increases with an increase in acceleration or a decrease in weight in water.

V. Conclusion

This paper presents the mathematical model of an underwater crawler system for investigating the dynamic effects on the vehicle's motion. Experiments were conducted for an ROV to climb over a bump in a water tank and to determine the slip characteristics at sea.

The simulated results for climbing over a bump agreed well with the experimental results. However, the two sets of results did not agree in the last stage of climbing over the bump. This may be due to the fluid dynamic interaction effect between the vehicle and the seafloor and the influence of the drive motor control system. These effects should be considered in the mathematical model for further improvement of the simulation.

For the slip characteristics on a seafloor, the calculated results again agree well with the experimental results. The shear stress distribution under the crawler belt varies in time and space, and a dynamic analysis is useful for understanding slip phenomena.

Thus, the dynamic analysis is important for understanding the motion of crawler-type ROVs, and the mathematical model presented in this paper is useful for a dynamic analysis, although the computer code needs further improvement for more accurate results.

Fig. 17. Photos of experiments on different seafloors using different-sized flipper-type crawler ROVs.

As part of future work, larger flipper-type crawlers have been developed [23], and experiments are currently being conducted to further verify the theory as well as observe the mobility of the flipper-type crawler on sandy seafloor, rock reefs with inclinations of up to 40°, and a seafloor covered with cobble and gravel (see Fig. 17) [23]. Development of an advanced crawler ROV will proceed to expand the activities.

References

[1] T. Inoue, H. Osawa, K. Takagi, A. Asada, M. Mochizuki, T. Katsui, and S. Tsukui, "Hard rock coring at the steep terrain seafloor with the flipper crawler ROV," in *Proc. Underwater Intervention Conf.*, New Orleans, LA, 2012, CD-ROM.

[2] T. Hirabayashi, T. Yamamoto, H. Yano, and H. Iwata, "Experiment on teleoperation of underwater backhoe with haptic information," in *Proc. Int. Symp. Autom. Robot. Construc.*, 2006, pp. 36–41.

[3] C. R. Deepak, M. Pugazhaandi, S. Paul, M. A. Shajahan, G. Janakiraman, M. A. Atmanand, K. Annamalai, R. Jeyamani, M. Ravindran, E. Schulte, J. Panthel, H. Grebe, and W. Schwarz, "Underwater sand mining system for shallow water," in *Proc. 3rd ISOPE Ocean Mining Symp.*, Goa, 1999, pp. 78–86.

[4] E. Shulte, H. Grebe, R. Handschuh, J. Panthel, B. Wenzlawski, W. Schwarz, M. A. Atmanand, C. R. Deepak, R. Jeyamani, M. A. Shajahan, and M. Ravindran, "Instrumentation and control system of a sand mining system for shallow water," in *Proc. 4th ISOPE Ocean Mining Symp.*, Szczecin, Poland, 2001, pp. 108–114.

[5] S. Wood, "Modular amphibious research crawler—Characterization of the coastal environment using a portable remotely operated vehicle," *Sea Technol.*, pp. 71–77, Feb. 2006.

[6] C. Bernstein, M. Connolly, M. Gavrilash, D. Kucik, and S. Threatt, "Demonstration of surf zone crawler: Results from AUV Fest 01," in *Proc. 5th Int. Symp. Technol. Mine Problem*, Monterey, CA, 2002, CD-ROM.

[7] T. Aponick and C. Bernstein, "Countermine operations in very shallow water and surf zone: The role of bottom crawlers," in *Proc. IEEE OCEANS Conf.*, San Diego, CA, 2003, pp. 1931–1940.

[8] T. Inoue, K. Takagi, and T. Shiosawa, “Flipper-type crawler system for running on the irregular seafloor,” in *Proc. IEEE OCEANS Conf.*, Sydney, Australia, 2010, DOI: 10.1109/OCEANSSYD.2010.5603541.
[9] T. Inoue, T. Katsui, H. Murakami, and K. Takagi, “Crawler system for the deep sea ROVs,” *MTS J.*, vol. 43, no. 5, pp. 97–104, 2009.
[10] M. Abe, H. Ito, C. Nakagawa, and K. Kobayashi, “Dynamic interaction between crawler shoes and road (1st report),” *Jpn. Soc. Mech. Eng.*, vol. 59, no. 560, pp. 1075–1079, 1993.
[11] T. Muri, “Terranechanics,” in *Gihodo-Shuppan* (in Japanese). Tokyo, Japan: Gihodo-Shuppan.
[12] D. M. Welling and D. B. Edwards, “Multiple autonomous underwater crawler control for mine reacuisition,” in *Proc. ASME Int. Mech. Eng. Congr. Expo.*, Orlando, FL, 2005, pp. 257–262.
[13] D. Welling, D. Edwards, and M. Anderson, “Fuzzy logic control for an autonomous underwater crawler,” in *Proc. ASME Design Eng. Tech. Conf./Comput. Inf. Eng. Conf.*, Salt Lake City, UT, 2004, pp. 715–721.
[14] K. Yoshida, K. Nagatani, Y. Okada, and D. Endo, “Trajectory control of crawler type mobile robot with consideration of a slip,” in *Proc. JSME Conf. Mechatron.*, Akita, Japan, 2007, pp. 2P1–L01.
[15] D. Endo, K. Nagatani, and K. Yoshida, “Improvement of dead-reckoning accuracy of crawler-type mobile robot by considering its slippage,” in *Proc. Annu. Conf. Robot. Soc. Jpn.*, Okayama, Japan, 2006, p. 2G17.
[16] T. Inoue, T. Katsui, J. Tahara, K. Itoh, H. Yoshida, S. Ishibashi, and K. Takagi, “Experimental research on movability characteristic of crawler driven ROV,” in *Proc. IEEE/MTS OCEANS Conf.*, Quebec City, QC, Canada, 2008, DOI: 10.1109/OCEANS.2008.5151802.
[17] T. Katsui, H. Murakami, S. Kajikawa, and T. Inoue, “Moving performance of crawler driven ROV on the inclined sea bottom,” in *Proc. ASME 30th Int. Conf. Ocean Offshore Arctic Eng.*, Shanghai, China, 2010, DOI: 10.1115/OMAE2010-20251.
[18] T. Katui, M. Akashi, S. Kajikawa, and T. Inoue, “The motion characteristics of crawler driven ROV moving over bump,” in *Proc. ASME 30th Int. Conf. Ocean Offshore Arctic Eng.*, Rotterdam, The Netherlands, 2011, DOI: 10.1115/OMAE2011-49801.
[19] T. Inoue, T. Katsui, H. Murakami, and J. Tahara, “Preliminary research on the thruster assisted crawler system for a deep-sea ROV,” in *Proc. IEEE OCEANS Conf.*, Bremen, Germany, 2009, DOI: 10.1109/OCEANSE.2009.5278293.
[20] T. Shiosawa, K. Takagi, and T. Inoue, “Experimental and theoretical study on the motion of ROV with crawler system,” in *Proc. IEEE/MTS OCEANS Conf.*, Seattle, WA, 2010, DOI: 10.1109/OCEANS.2010.5664332.
[21] T. Inoue, T. Shiosawa, and K. Takagi, “Dynamic motion of crawler-type ROV,” in *Proc. Under Water Technol.*, Tokyo, Japan, 2011, DOI: 10.1109/UT-2011-5774147.
[22] M. G. Bekker, *Theory of Land Locomotion*. Ann Arbor, MA: Univ. Michigan Press, 1956, ch. VII.
[23] T. Inoue, K. Takagi, and T. Shiosawa, “Experiments of flipper type crawler system at sea to verify running performance on sandy or irregular steep terrain seafloor,” in *Proc. IEEE OCEANS Conf.*, Santander, Spain, 2011, DOI: 10.1109/Oceans-Spain.2011.6003419.

Tomoya Inoue (M'10) received the B.Sc. and M.Sc. degrees from Osaka University, Osaka, Japan, in 1993 and 1995, respectively, and the Ph.D. degree from the Tokyo University of Marine Science and Technology, Tokyo, Japan, in 2010, all in ocean engineering.

From 1995 to 2001, he worked at Hitachi Zosen Corporation, as an Engineer and a Chief Engineer for an offshore project. Since 2002, he has been a Senior Research Scientist at the Japan Agency Marine-Earth Science and Technology (JAMSTEC), Yokohama, Kanazawa-ku, Japan. His research interests are in offshore deep drilling technology and underwater vehicle.

Dr. Inoue is a member of the IEEE Oceanic Engineering Society (OES) and a member of the Japan Society of Naval Architects and Ocean Engineers. He was awarded the IEEE OES Japan Chapter Young Researcher Award in 2010.

Takuya Shiosawa received the B.Sc. degree from Osaka University, Osaka, Japan, in 2009 and the M.Sc. degree from The University of Tokyo, Tokyo, Japan, in 2011, both in ocean engineering.

Since 2011, he has been an Engineer with Kawasaki Heavy Industries.

Ken Takagi (M'04) received the B.Sc., M.Sc., and Dr.Eng. degrees from Osaka University, Osaka, Japan, in 1982, 1984, and 1989, respectively.

From 1985 to 2008, he was an Assistant Professor and an Associate Professor for Naval Architecture and Ocean Engineering at Osaka University. Since 2008, he has been a Professor for Ocean Technology, Policy, and Environment with The University of Tokyo, Tokyo, Japan. His research interests are in marine renewable energy and underwater vehicle.

Dr. Takagi is a member of the IEEE Oceanic Engineering Society.